

# We are IntechOpen, the world's leading publisher of Open Access books Built by scientists, for scientists

6,900

Open access books available

185,000

International authors and editors

200M

Downloads

Our authors are among the

154

Countries delivered to

TOP 1%

most cited scientists

12.2%

Contributors from top 500 universities



WEB OF SCIENCE™

Selection of our books indexed in the Book Citation Index  
in Web of Science™ Core Collection (BKCI)

Interested in publishing with us?  
Contact [book.department@intechopen.com](mailto:book.department@intechopen.com)

Numbers displayed above are based on latest data collected.  
For more information visit [www.intechopen.com](http://www.intechopen.com)



# Methodologies for Achieving 1D ZnO Nanostructures Potential for Solar Cells

*Yeeli Kelvii Kwok*

## Abstract

One-dimensional (1D) nanostructures are generally used to describe large aspect ratio rods, wires, belts, and tubes. The 1D ZnO nanostructures have become the focus of research owing to its unique physical and technological significance in fabricating nanoscale devices. When the radial dimension of the 1D ZnO nanostructures decreases to some lengths (e.g., the light wavelength, the mean of the free path of the phonon, Bohr radius, etc.), the effect of the quantum mechanics is definitely crucial. With the large surface-to-volume ratio and the confinement of two dimensions, 1D ZnO nanostructures possess the captivating electronic, magnetic, and optical properties. Furthermore, 1D ZnO nanostructure's large aspect ratio, an ideal candidate for the energy transport material, can conduct the quantum particles (photons, phonons, electrons) to improve the relevant technique applications. To date, many methods have been developed to synthesize 1D ZnO nanostructures. Therefore, methodologies for achieving 1D ZnO nanostructures are expressed, and the relevant potential application for solar cells are also present to highlight the attractive property of 1D ZnO nanostructures.

**Keywords:** ZnO, one dimensional, nanostructures, chemical vapor transport and condensation (CVTC), chemical vapor deposition (CVD), metal-organic chemical vapor deposition (MOCVD), vapor-liquid-solid (VLS), hydrothermal, electrochemical, solar cell

## 1. Introduction

To date, nanotechnology is the operation of matter on an atomic and molecular scale. Generally speaking, the size scale in nanotechnology including materials, devices, and other structures is at least from 1 to 100 nanometers in one dimension. The revolution of the nanotechnology is taking a crucial effect on the different fields, such as commercial sectors, engineering, science, drug delivery, sensors, and the construction industry. Nanostructures in such size have made steadily increasing attraction because of their attractive and captivating properties, same as their fascinating applications complementary to the materials in bulk. The interesting properties of materials in nanoscale (both physical and chemical) can make the efficacy enhanced distinctively in mechanical strength, (photo)catalysis, optical sensitivity, and (thermal and electrical) conductivity which enable applications such as improved materials with higher properties, storage devices of the electronic and energy, sensors, and catalysts [1–8].

According to the dimensions in nanometer scale size, nanostructures can be classified into the following three groups:

- a. Zero-dimensional (0D) nanostructures (quantum dots, nanoparticles, or nanoclusters)
- b. One-dimensional (1D) nanostructures (nanowires, nanorods, nanotubes, nanoribbons, nanobelts, or nanocables)
- c. Two-dimensional (2D) nanostructures (super-thin films, multiple-layer films, or superlattices)

In comparison with 0D nanostructures, it is easier to investigate the relationship between the mechanical properties, optical and electronic transport, and the confinement of the size and dimensionality for 1D nanostructures. Moreover, 1D semiconductor nanomaterials have an extremely crucial effect of the active components and interconnect in the nanoscale electronic and photonic devices fabrications.

Up to now, 1D nanostructure is generally used to describe large aspect ratio rods, wires, tubes, and belt and tubes and has been the key point of investigation due to its attractive physical and technological significance in fabricating nanoscale devices. When the radial diameter of the 1D nanostructure is lower than some lengths (the path of the phonon mean free, the light of wavelength, Bohr radius, etc.), the effect of the quantum mechanics will be crucial. Owing to the large surface-to-volume ratio and the confinement of two dimensions, nanowires possess the definitely attractive electronic, magnetic, and optical properties. In addition, because nanowires' aspect ratio is extremely large, the quantum particles (photons, phonons, electrons, etc.) can be conducted directly easily to make the nanowires as the ideal candidate for the energy transport materials to enhance the relevant technique applications [9–17].

Today, numerous approaches have been researched to synthesize 1D nanostructures. Two fundamental steps are essentially involved in the evolution: nucleation and growth. A lot of solid materials with 1D nanostructures in nature are controlled by the bonding in the structure of crystallography in the highly anisotropic. The materials need common growth conditions including chemical vapor deposition (CVD), wet-chemical routes, and template-assistant methods. In classification, all the contemporary approaches are divided into bottom-up and top-down methods. The most important issue for developing a new synthetic method is to control the dimensions, morphology, and uniformity of nanostructures. When making a method to synthesize the nanostructures by the synthetic effects, it is definitely important to control the related morphology (or shape), dimensions, and uniformity simultaneously. To obtain 1D growth nanostructures, several chemical methods were generated. The current common six different strategies are (1) the reduction of a 1D microstructure in size, (2) 0D nanostructure self-assembly, (3) by a capping reagent kinetic control, (4) a template usage for direction, (5) a liquid droplet confinement as in the vapor-liquid-solid process, and (6) the control of a solid with the anisotropic crystallographic structure.

Generally, there are four popular mechanisms for understanding the synthesis of 1D nanostructure materials. They are the mechanism of vapor-liquid-solid (VLS), the mechanism of oxide-assisted growth (OAG), the mechanism of vapor-solid (VS), and the mechanism of solution-liquid-solid (SLS).

### **1.1 Vapor-liquid-solid (VLS)**

In the VLS mechanism, a liquid metal cluster or catalyst, such as Au, Fe, Ni, or Co, is taken as the energetically favorable point of the gas-phase reactant absorption.

The reactant supersaturates and segregates from the cluster and then grows into a 1D structure of the material, the diameter of which is limited by the size of the liquid metal catalyst that can be achieved under equilibrium conditions [18–21].

### **1.2 Oxide-assisted growth (OAG)**

This kind of the synthesized technique, in which oxides replaced by metals have a crucial effect on the nucleation induction and the nanowire growth, can produce the high-purity 1D nanomaterials in the large quantities, and the metal catalysts do not need any more. The 1D nanomaterial synthesis with the mechanism of the oxide-assisted growth is the extension of the traditional vapor-liquid-solid method with the metal catalyst. Moreover, it can be taken to make the nanowires by other materials than silicon [22–26].

### **1.3 Vapor-solid (VS)**

For the mechanism of the vapor-solid (VS), the size of the nucleation site is critical for defining the rod diameter when the vapor supersaturation is appropriately controlled. Metal catalysts are not necessary. Three stages can be summarized as the illustration: (i) The source forms vapor phase, (ii) the vapor is transported by the carrier gas and deposits on the substrate to form crystalline nuclei, and (iii) the defects of the nuclei become the growth points, and the reactive vapor molecules further grow into nanostructures [27, 28].

### **1.4 Solution-liquid-solid (SLS)**

Solution-liquid-solid (SLS) phases are involved in the nanowire growth that is in fact an analogy to the conventional whisker growth via vapor-liquid-solid (VLS) mechanism. The difference is that the vapor phase involved in the VLS growth is now substituted by a solution phase in the SLS mechanism. In turns out, however, the nanowires prepared by the SLS mechanism have a varying diameter ranging from 10 to 150 nm, which is not uniform [29, 30].

## **2. Property of one-dimensional (1D) nanomaterials**

Up to now, it is still a challenge to accurately characterize the property of 1D nanostructures due to the constrains of the current measuring techniques, such as (1) the size of 1D nanostructures is too small to adopt the well-established testing techniques and (2) 1D nanostructures different from bulk materials are hard to pinpoint at the desired location. Therefore, the relevant techniques should be explored to detect the property of 1D nanostructures accurately.

### **2.1 Mechanical property**

1D nanomaterials behave qualitatively different from the conventional bulk materials when the size reduces to nanoscale. It is well known that the increments of yield stress and the hardness of a polycrystalline material are consistent with the decrement of the grain size to the micrometer scale, and this significant phenomenon is defined as the Hall-Petch effect. For the single-crystalline 1D nanostructures, their property is extremely higher than that of the counterparts in the larger dimensions.

## 2.2 Thermal property

For 1D nanostructures, the great reduction of the melting point of a solid material is very obvious. Because of the special characteristics of nanocrystal materials, the high specific boundary area means large stored interface energy. Consequently, 1D nanostructures can be tailored precisely on the basis of their thermal property, such as synthesizing and annealing temperatures [31–33].

## 2.3 Electronic property

For 1D nanostructures, the grain size and boundaries are the dominated factors effected on the electron mean free path and resistance. There is a trend that many physical properties of 1D nanostructures like optical, magnetic, and electrical properties will be enhanced distinctively when the size or dimension of the material reduces to nanosize ( $\sim 10^{-9}$  m) scale. Moreover, such 1D nanostructures (such as nanowires, nanorods, etc.) are generally prone to be enriched with many surface defects and oxygen and cation vacancies due to their low formation energy within nanoscale materials [34, 35].

## 2.4 Magnetic property

Magnetic properties of materials are fundamentally determined by the magnetic couplings at the atomic level. Unlike bulk ferromagnetic materials, which usually form multiple magnetic domains, 1D nanomaterials consist of the simple magnetic domain resulted in obvious difference in several important aspects from the property of their bulk counterparts [36–40].

## 2.5 Optical property

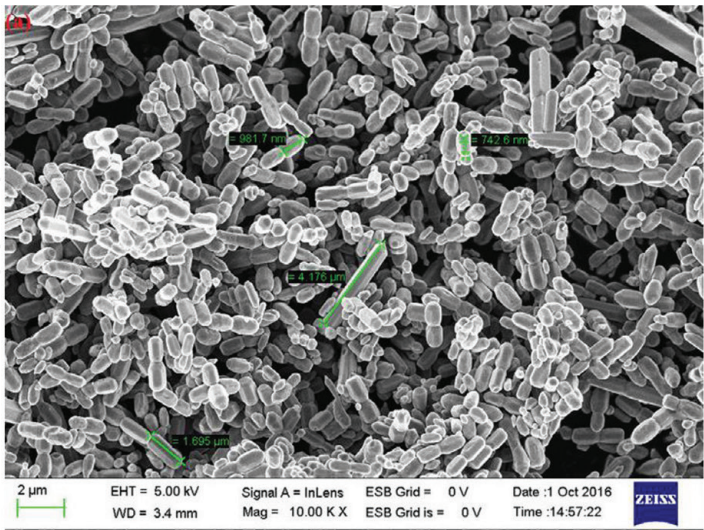
The confinement of the size has a significant effect on the energy levels of the nanowire determination when its diameter decreases to some critical length (Bohr radius). Results indicate that the nanowire absorption edge of silicon is obviously blue-shifted because the bulk silicon indirect bandgap is only 1.1 eV. The characteristics of the absorption spectra are sharp and discrete along with the photoluminescence (PL) in the relatively strong “band-edge.” At the same time, along the longitudinal axes of the nanowires, the emitted light is highly polarized [41–44].

## 3. Zinc oxide

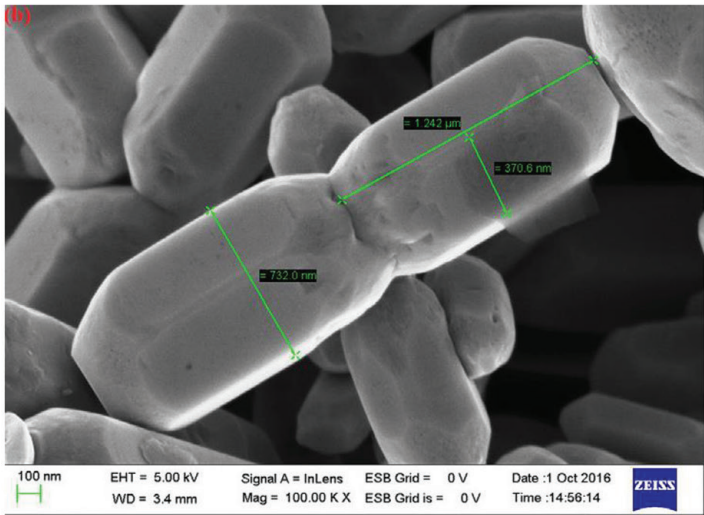
Zinc oxide (ZnO) has been investigated for a long time as it is an amazing material with multiple functions. ZnO is a direct wide bandgap semiconductor material with piezoelectric and photoelectric properties. ZnO has a wide direct bandgap of 3.37 eV which is similar to GaN and a high exciton binding energy of 60 meV at room temperature. The wide bandgap gives good optical transparency to visible light which makes ZnO a suitable candidate for short wavelength photonic applications (UV and blue spectral range). ZnO has a non-central symmetric wurtzite structure, and the relevant hexagonal unit cell ( $a = 3.25 \text{ \AA}$ ,  $c = 5.20 \text{ \AA}$ ) packed  $\text{O}^{2-}$  closely and stacked  $\text{Zn}^{2+}$  layers alternately along the  $c$ -axis direction. Due to the unique fascinating property in electronics, optics, photonics, and magnetics, ZnO provides an impact on applications in various areas, such as solar cells, supercapacitors, sensors, catalysis, light-emitting, actuators, and biomedical devices. ZnO has equal importance in relation to silicon-based 1D nanostructures in the field of 1D



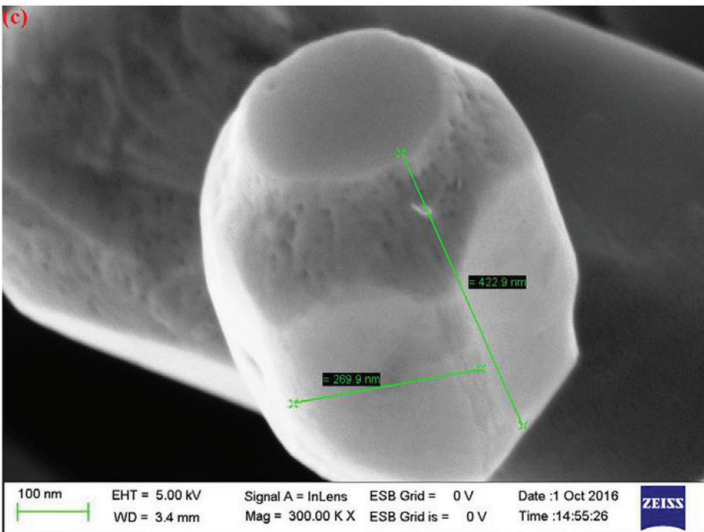
nanostructures, and it has an increasing influence in developing nanotechnology. To date, various quasi-one-dimensional nanostructures of ZnO have been synthesized, i.e., nanowires, nanobelts, and nanotubes [45–47]. **Figure 1(a–c)** expresses the images of ZnO rods taken by SEM synthesized at pH 8. It indicates that the length



(a)



(b)



(c)

**Figure 1.**  
(a–c) ZnO nanorod images taken by SEM synthesized at pH 8 (a) 10 k×, (b) 100 k×, and (c) 300 k×.

of synthesized ZnO nanorods is about 4  $\mu\text{m}$  with the diameter of around 700 nm and ZnO nanorods with the flat top surface, and they stack one by one through polar surfaces. From the crystal structure of the ZnO, the ions of Zn and O are arranged alternatively through  $c$  axis where the bottom surface is  $\text{O}^{2-}$  terminated (000-1) and the top surface is  $\text{Zn}^{2+}$  terminated (0001). The surfaces of the flat top explored in the nanorods of ZnO are contributed to the polar surface disappearance. In the basis solution with the weak volume, the precipitate of  $\text{Zn}(\text{OH})_2$  solid exists in the reactant solution. Owing to the dipole interaction,  $\text{Zn}(\text{OH})_2$  solid is taken as the polar surface that could easily make the positive and negative surfaces of ZnO crystal incorporate efficiently. Therefore, the surface energy of the polar surfaces is relatively high than that of the nonpolar surfaces, disappears at the first when the nonpolar surfaces start to slowly grow, and appears in the last stage of ZnO nanostructure crystal growth [48].

#### 4. Methodologies for achieving 1D ZnO nanostructures

ZnO nanostructures have already been synthesized by various methods. There are mainly two methods to prepare 1D ZnO according to the state-of-growth medium: vapor phase process and liquid phase process. The vapor phase method includes chemical vapor deposition (CVD), metal-organic chemical vapor deposition (MOCVD), molecular beam epitaxy (MBE), pulsed laser deposition (PLD), etc. The liquid phase method includes hydrothermal method, electrochemical method, sol-gel method, and so on. The growth mechanism can be classified into mainly three categories: vapor-solid (VS) growth, vapor-liquid-solid (VLS) growth, and solution-liquid-solid (SLS) growth.

##### 4.1 Chemical vapor transport and condensation (CVTC)

The chemical vapor transport and condensation (CVTC) method is processed in a tube furnace. The substrates coat with a layer of Au thin film with thermal evaporation methods to control the thickness of the film in the CVTC system. ZnO powder and graphite powder in the same amounts are mixed together and milled effectively; then put them into a boat made by alumina. Then, the alumina boat and the substrate with Au film are placed into a small quartz tube. Usually, the substrates are kept 5–10 cm away from the alumina boat center. At the furnace center, the boat of the alumina sits, and at the downstream of the argon flow, the substrates are positioned. The system is raised to 800–900°C and maintained for 5–30 min. Light or dark gray materials are attained on the surface of the substrate.

The transmission electron microscope (TEM) image of an alloy tip on a thin nanowire is shown in **Figure 2**. According to the features of the alloy tip, it indicates a clear growth procedure by vapor-liquid-solid (VLS) growth mechanism. The synthesized tips of nanowires shown in **Figure 2a** are grown by both the hydrogen and graphite reduction approaches. The relevant high-resolution transmission electron microscope (HRTEM) image of a single-crystalline ZnO nanowire is shown in **Figure 2b**. It expresses that the space of the adjacent lattice planes of  $2.56 \pm 0.05 \text{ \AA}$  is consistent to the distance of two crystal planes in (002). Consequently, it indicates that the growth direction for the ZnO nanowires is  $\langle 001 \rangle$ . Meanwhile, it is also observed in the high diffraction intensity of (001) peaks of XRD results to confirm that the preferential growth direction is  $\langle 001 \rangle$  [49, 50].

**Figure 3** expresses a representative image of a patterned ZnO nanowire synthesized on silicon (Si) substrate with the patterned Au islands taken by scanning electron microscopy (SEM). The diameters of the nanowires are from 20 to 120 nm,



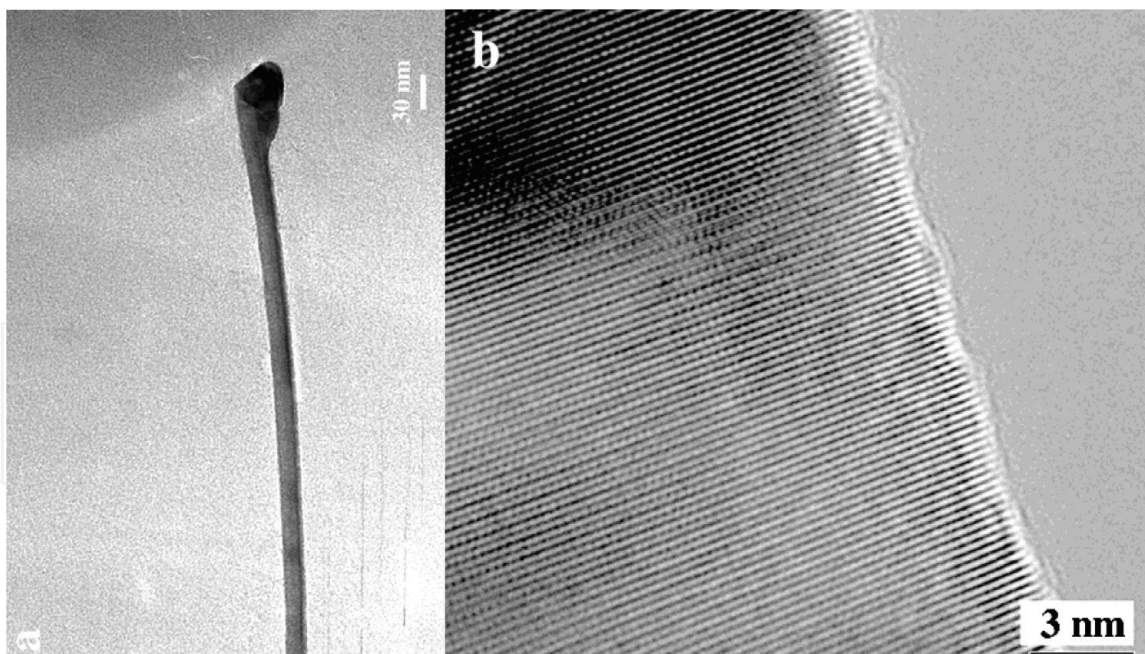


**Figure 2.**  
(a) A thin ZnO nanowire image taken by TEM with a Zn/Au alloy tip. (b) the lattice fringes of high-resolution TEM image of a single-crystalline ZnO nanowire.

and the length is 5–20  $\mu\text{m}$ . The directions of the grown nanowires on (100) Si substrate are random.

SEM results show that the flexible, long, fine ZnO nanowires grow extensively from the hexagons' edges. The growth of nanowires is consistent with the copper grid in the hexagonal pattern abundantly. Interestingly, a complicated intricate network is formed due to lots of the nanowires connecting with the neighboring metal hexagons. SEM images for the higher magnification of the same sample illustrate more detailed particulars as shown in **Figure 3b**.

ZnO NWs grown under the vapor-liquid-solid process begin together with the reductive Zn gaseous reactants dissolution into the Au catalyst liquid droplets in nano-size, and then the alloy metal is formed followed by the supersaturation of Zn along with the single-crystalline wire growth. The schematic growth mechanism is expressed in **Figure 4**. In this method, the diameter, density, and location of ZnO NWs can be controlled according to the desired characteristics. As a result, ZnO NWs with the required properties can be attained and tailed successfully. However, the metal catalyst affects the purity of the product which can lower the performance of the nanowires [51–56].

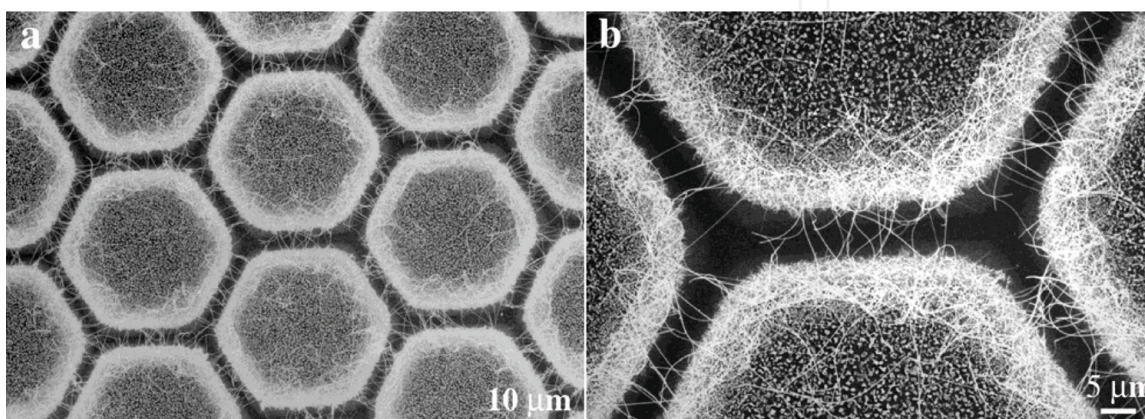


**Figure 3.**  
(a) From the patterned Au islands images of ZnO nanowire networks synthesized taken by SEM. (b) Higher magnification SEM image for the same sample.



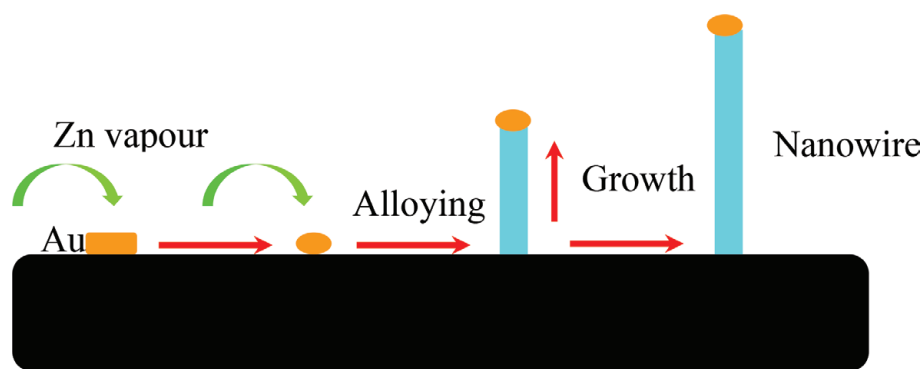


**Figure 4.**  
Schematic mechanism of ZnO NW growth.

## 4.2 Chemical vapor deposition (CVD)

The aligned 1D ZnO NWs fabricated by patterning metal catalytic particles through VLS growth involve tedious lift-off processes for patterning metal catalysts and may lead to serious contamination in complementary metal oxide semiconductor processing. To avoid the effects of the catalyst, CVD without the catalyst has been developed. The zinc oxide NW growth is proceeded and developed earlier when the flow-type reactor is at a reduced pressure of the elemental vapor phase synthesis. Highly purified metallic granulated Zn (99.99%) is placed in the boat made by the alumina. After that, it is inserted at a quartz ampoule end which is sealed at one end. Meantime, a wide slit in the ampoule is at the open end. The substrates are mounted with their front sides up and below the ampoule. Then, a horizontal two-zone flow-type quartz reactor is used for putting the ampoule inside in order to make sure that the source of zinc is situated in one of the zones (evaporation zone), the substrates, and in the other (growth zone). The arrays of ZnO growth are very allergic to the processing parameters, especially for the well-aligned nanorods. Wang ZL and his co-workers firstly fabricated a ZnO nanobelt in 2001 using catalyst-free CVD methods and applied it to the devices [57]. Furthermore, Wang's group also achieved the formation process of a rectangular cross section by simply evaporating ZnO powder at elevated temperatures. The structures of as-synthesized nanobelts are uniform. Most of the nanobelts are single crystals and free from defects and dislocations. To obtain the ZnO nanowire arrays (NWAs) via catalyst-free CVD methods, many groups have adopted different methods to reach the objective [58–62]. One method is to adopt a ZnO film layer to induce the growth of ZnO NWs. The nucleation stage of ZnO nanocrystals plays an important role. Firstly, the zinc metal droplet condenses on the surface of the substrate due to the different heating temperatures in the evaporation and growth zones. The diameter of catalyst droplets can be controlled by zinc and oxygen partial pressure which is different from the Au catalyst growth mechanism. In addition, Menzel A et al. deeply investigated the method for tuning the growth mechanism of ZnO nanowires under the various conditions and put out the related parameters for a controlled NW growth by CVD method to change the nanowire shapes. The results are shown in **Figure 5** [63].

## 4.3 Metal-Organic chemical vapor deposition (MOCVD)

The MOCVD method, apart from its increasing advantages because of its unique characters of the industry, has been illustrated to be effectively taken to ZnO NW synthesis with good controllable shape, high quality, and reproducibility. The growth of ZnO NWs with high quality by catalyst-free MOCVD was explored firstly by Park et al. [64]. After that, the huge effort has been put into the field of

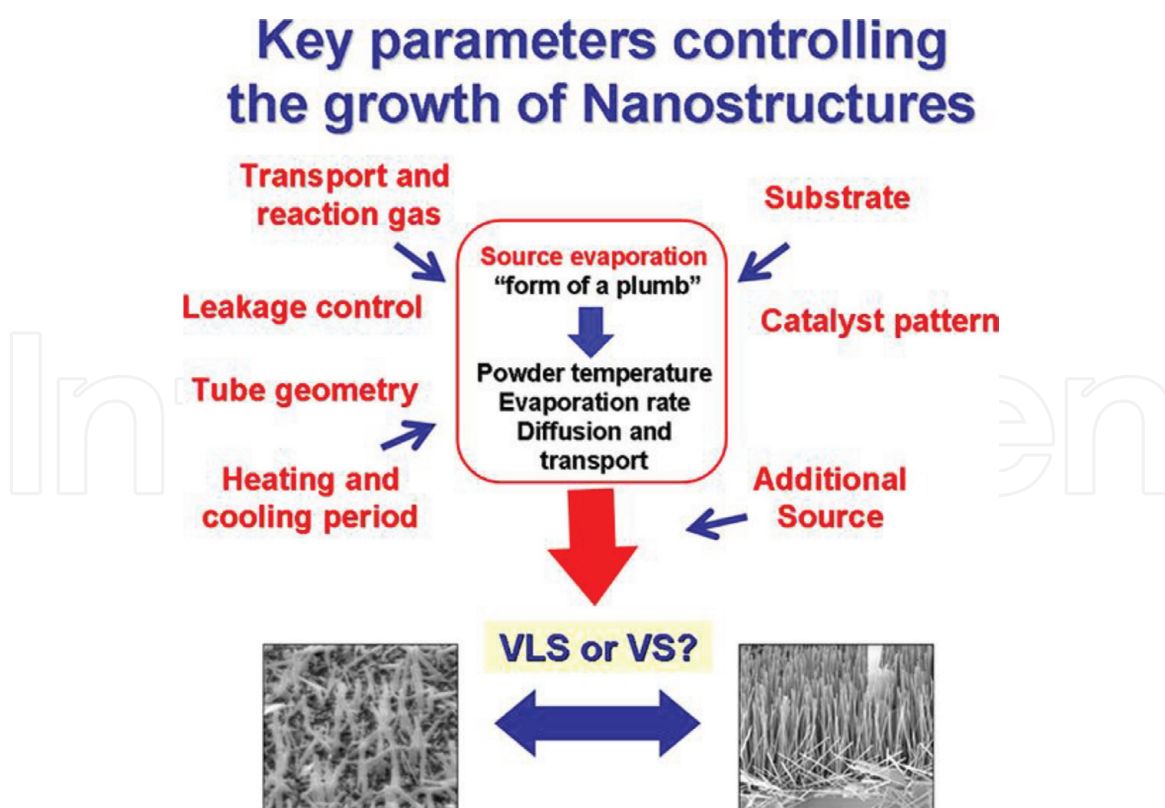


**Figure 5.**  
Schematic diagram of the key parameters controlling the NW growth.

the synthesis of the ZnO nanostructures, and great progress has subsequently been obtained [65–69]. Up to now, the contributions relevant to MOCVD growth of ZnO nanostructures, diethylzinc (DEZn), dimethylzinc (DMZn) as zinc precursor, nitrogen or argon as carrier gas, and low reactor-pressures have been mostly used. Park's group reported the growth of ZnO NWs, which requires no metal catalysts. The nanorod growth temperature was as low as 400°C. However, the preparation machine and source materials are more expensive than other methods which have hindered its practical applications.

#### 4.4 Chemical solution method

Chemical solution deposition is one of the commonly employed synthesis methods for ZnO nanostructures, particularly in large-scale fabrication for device purposes [70–75]. Chemical reactions between different precursors play a key role in the synthesis. The advantages of the solution method include the economical synthesis, the large scale, and the low temperature. For ZnO nanomaterials growing on a substrate, the approaches of solution mostly adopt the hydrothermal procedure by a kind of solution in an aqueous which includes an organic amine and zinc salt. In addition, in order to enhance the ZnO NR alignment on the substrate, a textured ZnO nanocrystal or a ZnO thin film is taken as a seed layer.

In a typical chemical solution synthesis, a layer of ZnO seed layer is spread over a Si substrate by dipping or sputtering. This kind of seeding method is simply suitable for different substrates. The ZnO seed layer thickness is usually 10–200 nm. A calculated amount of zinc nitrate hexahydrate is dissolved in 80 mL deionized water to obtain 1–40 mM solutions for growth solution preparation. Then, the pH of the solution for ZnO growth is adjusted by ammonia water addition. The amount of the ammonia water addition related to the target pH and the zinc salt concentration is usually about 0.1–5 mL. The growth of the hydrothermal ZnO NRs is explored

with Zn/Si substrate suspended upside down in a kind of Teflon-capped glass bottle which is full of the growth solution. The temperature of ZnO growth ranges from 60 to 90°C and the reacting time is 6 h. When the synthesis is finished, the substrate is taken from the reactant solution. At the same time, the substrate is rinsed by the DI water and dried successively. Therefore, the morphology (length, diameter) of the synthesized nanorods relied on the relevant parameters, for instance, zinc seed layer morphology, pH, growing temperature, and zinc salt concentration.

**Figure 6a** shows ZnO nanorods viewed normal to the surface grown by the two-step chemical bath deposition process, in which the facets are exactly crystal-line hexagonal and its average ratio of the aspect is about  $3 \pm 1$  [76]. **Figure 6c** illustrates the sulfidation of ZnO nanorods with definitely well particle decoration of the entire surface of ZnO nanorods, and the end and side of facets are not in the well-defined morphology. With the reaction increasing, a more uniform film coated

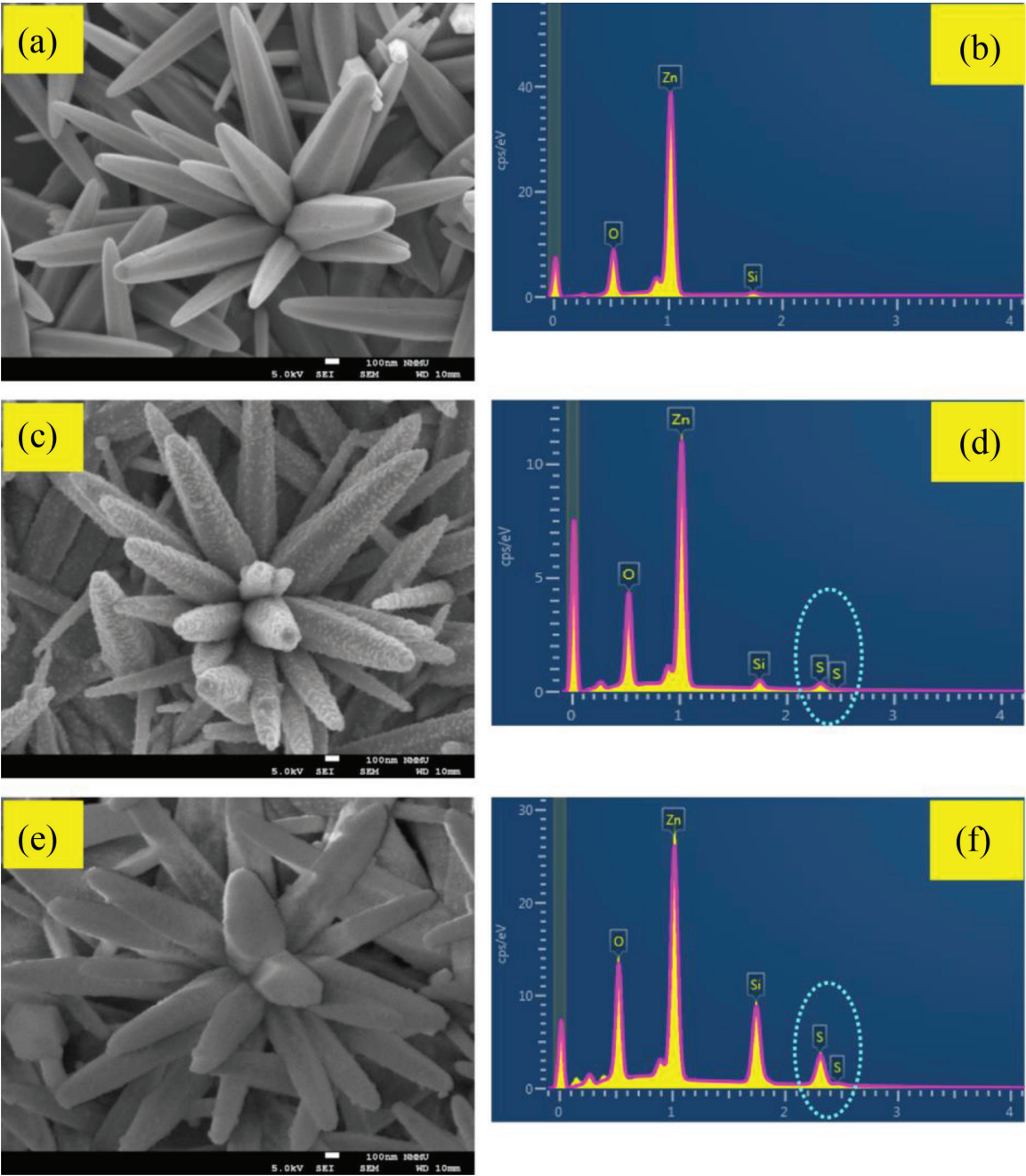


**Figure 6.** ZnO nanorod (a) initial morphology (sample A) before sulfidation, (c) sulfidation for 90 min at 75°C in 160 mmol Na<sub>2</sub>S<sub>(aq)</sub> (sample B), and (e) treatment further for 90 min at 75°C in 160 mmol Zn(NO<sub>3</sub>)<sub>2</sub>·6H<sub>2</sub>O<sub>(aq)</sub> (sample C). EDS image (b) results of a, (d) results of c, and (f) results of e.



on ZnO nanorods can be easily observed as shown in **Figure 6e**. Moreover, the side and end facets of the synthesized ZnO nanorods as shown in **Figure 6e** become more smooth (cf. **Figure 6a**, **Figure 6c**, and **Figure 6e**). Meanwhile, EDX results agree well with the relevant SEM results.

The related TEM results are shown in **Figure 7**. It expresses that ZnO nanorod is coated with an uneven film. The selected area diffraction (SAD) result as shown in

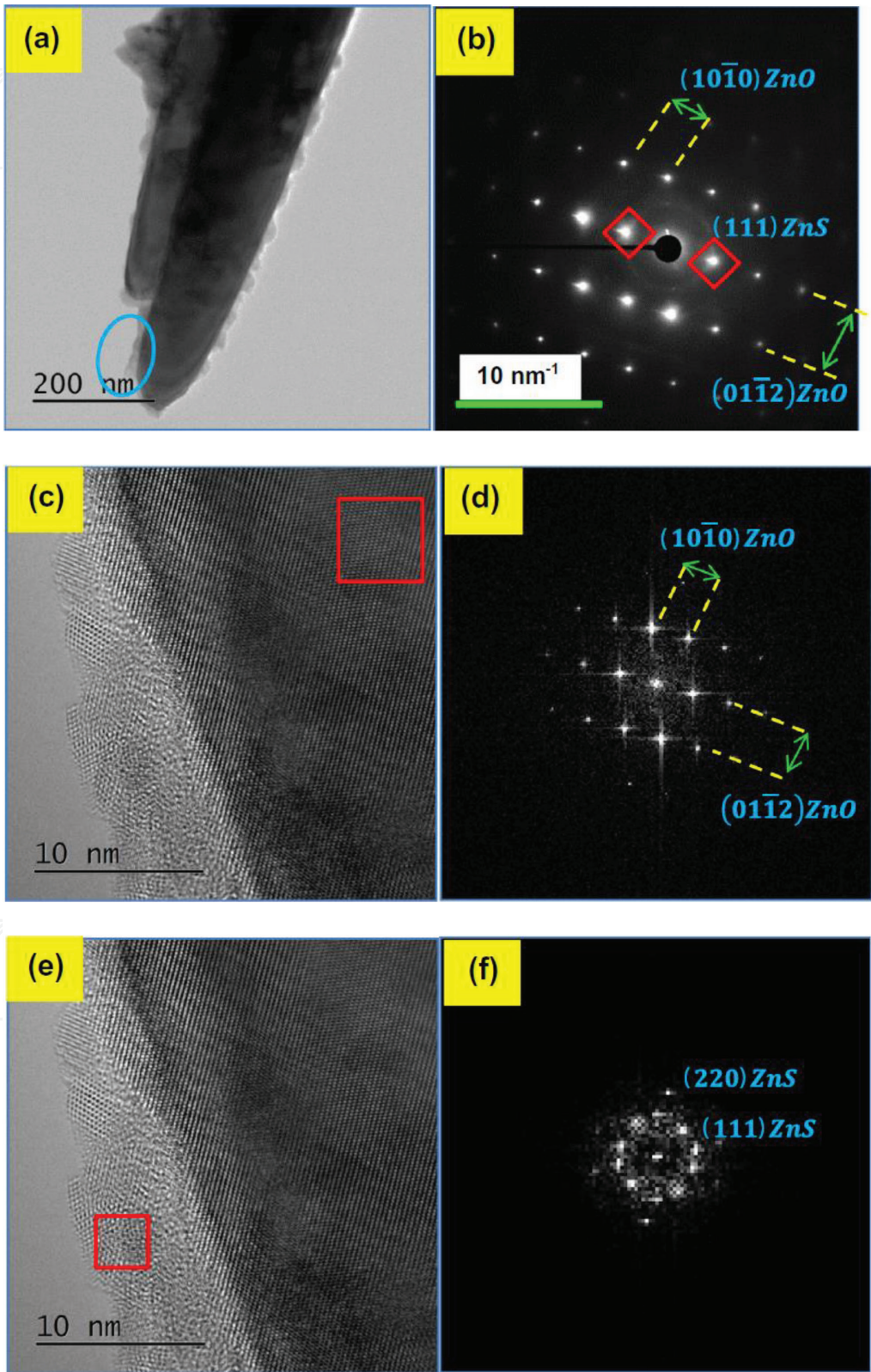


**Figure 7.** Sample B images of HRTEM. (a) Sulfidation nanorod (bright field), (b) region in blue ellipse (**Figure 7a**) (selected area diffraction (SAD) pattern), (c and e) interface of ZnO-ZnS (high-resolution images), (d) region in red (**Figure 7c**) live Fourier transformation, and (f) region in red (**Figure 7e**) live Fourier transformation.

**Figure 7b** assures the crystalline structure in which the bright spots are the crystalline ZnO and the rings are the polycrystalline ZnS. The interplanar distances related to ZnO (01-12) and (10-10) and ZnS (111), together with the relationship of the partial epitaxial between ZnS shell and ZnO core where (10-10) ZnO// (111) ZnS, are confirmed. Furthermore, the calculated parameters of the lattice of ZnO core are  $5.35 \pm 0.01 \text{ \AA}$  at the *c*-axis and  $3.29 \pm 0.01 \text{ \AA}$  at the *a*-axis.

## 5. Solar cells

### 5.1 Advantages of ZnO NWs/NR arrays

ZnO has a large bandgap (3.37 eV) *n*-type semiconductor which can be easily synthesized into large-scale arrayed 1D ZnO structures and the patterning of them. The facile synthesized property and its natural characteristics make ZnO NRs a widely used template material in the field of sensitized solar cells and preparing nanotubes.

The attractive characteristic of ZnO is the superior electron mobility, which is more than one magnitude order larger than that of the anatase titanium oxide, in all of the semiconductors with the wide bandgap which are taken as replacements of titanium oxide for the electron conductor. ZnO NR-based solar cells are promising devices for solar energy conversion. Because NRs have strong light absorption and rapid carrier collection, in addition they are inexpensive due to the cheap element and small amount of material needed. Compared to planar solar cells, NR photovoltaic devices have enhanced optical absorption due to three effects. ZnO NRs can reduce reflectivity, and the incoming light is captured and confined into guided modes which lead to concentration of the electromagnetic field inside the absorbing material. Moreover, the nanowire arrays support the light along a diffusive path leading to multiple scattering between the wires.

### 5.2 Excitonic solar cells

Conventional solar cells are the silicon *p-n* junction type invented in the 1950s. Nevertheless, the cost of solar power is too high to be extended industrially. To reduce the cost, a great deal of research has been devoted to less expensive types of solar cell. One of the great promises is the emergence of excitonic solar cells. The difference between conventional and excitonic solar cells is that light absorption results in the formation of excitons in semiconductor materials rather than free electron-hole pairs. Excitonic solar cells consist of molecular semiconductor solar cells, conducting polymer solar cells, dye-sensitized solar cells (DSSCs) [77, 78], and quantum dot solar cells (QDSSCs) [79–82].

Among the different types of excitonic solar cells, the ZnO NR array is popular in the fields of DSSCs and QDSSCs. The dye-sensitized solar cell concept is on the basis of the dye optical excitation, and the conduction band with the metal oxide in the nanostructure wide bandgap is injected into an electron. At the beginning, a kind of the dye-sensitized cell made of a dense array of oriented, crystalline ZnO NWs was researched and attained with a full sun efficiency of 1.5%. To increase the efficiency of such cells, researchers have adopted different methods such as using alternative sensitizers and redox electrolytes to fabricate solid-state or nonvolatile-liquid DSSCs. The new record power conversion efficiency (PCE) in DSCs is 7%, adopted with the synthesized multilayer assemblies of high-surface-area ZnO NWs to fabricate DSSCs [83, 84].

However, despite the successes of DSSCs, novel hybrids of the architectures of device and materials are still hunting to further enhance solar cell performance and cost. Quantum dots (QDs) are one possibility to substitute photosensitive dyes.

Compared to dye, the particle size of QDs can be tuned for adjusting their absorption spectrum to match the solar spectrum better. Also, the efficiency of the photovoltaic (PV) device can be improved effectively by QDs which can make multiple electron-hole pairs per photon. The maximum thermodynamic conversion efficiency of QDSSCs can theoretically reach 44% which is much higher than for DSSCs. In 2007, Aydil ES's group demonstrated ZnO NWs with CdSe QDs photosensitization and provided proof of QDs photogenerating electron transfer to the nanowires for the first time. They proved the possibility of QDs that demonstrated ZnO NWs providing a promising solar cell architecture [85]. Most reported values of ZnO NWs' QDSSCs (typically below 3%) are well below DSSCs (7%). With the time flying, more research on ZnO NWs' QDSSCs keeps forward with the higher efficiency. The performances of QDSSCs are typically limited by problems of aggregation, low QD loading density, and high expense of synthesis to hinder its large-scale applications [86–88].

## 6. Conclusion

ZnO being one-dimensional (1D) nanostructures is playing an increasingly crucial role in the developing nanoscience and nanotechnology. Due to its unique physical and chemical properties, 1D ZnO nanostructures can definitely enhance remarkably the efficacy in optical sensitivity, (photo)catalysis, mechanical strength, and (thermal and electrical) conductivity, which is beneficial to electronic and energy storage devices, sensors, advanced mechanical materials, and catalysts. Nowadays, the state-of-art resources of the renewable alternative energy with the cutting-edge techniques are urgent to be explored to make them to play the crucial role in the energy consumptions for the future along with the eco-friendly to benefits of the environment and technics, especially considering on the basis of taking an ideal candidate for the traditional energy resources. Solar energy is the radiant energy that is produced by the sun. In many parts of the world, the direct solar radiation is considered to be one of the best prospective sources of energy with the highlighted environmentally friendly benefits. Therefore, the deep insight into the properties of 1D ZnO nanostructures shall be explored more and coupled with the relevant techniques of solar cells. Meanwhile, the methodologies for achieving 1D ZnO nanostructures eco-friendly or green to the environments shall be also researched further along with the relevant detailed mechanism revelation.


### Author details

Yeeli Kelvii Kwok

Department of Mechanical and Biomedical Engineering, City University of Hong Kong, Kowloon Tong, Kowloon, Hong Kong

\*Address all correspondence to: [yeelikwok@yahoo.com](mailto:yeelikwok@yahoo.com)

### IntechOpen

© 2019 The Author(s). Licensee IntechOpen. This chapter is distributed under the terms of the Creative Commons Attribution License (<http://creativecommons.org/licenses/by/3.0>), which permits unrestricted use, distribution, and reproduction in any medium, provided the original work is properly cited. 



## References

- [1] Rawtani D, Khatri N, Tyagi S, Pandey G. Nanotechnology-based recent approaches for sensing and remediation of pesticides. *Journal of Environmental Management*. 2018;**206**:749-762
- [2] Kesharwani P, Gorain B, Low SY, Tan SA, Ling ECS, Lim YK, et al. Nanotechnology based approaches for anti-diabetic drugs delivery. *Diabetes Research and Clinical Practice*. 2018;**136**:52-77
- [3] Contreras JE, Rodriguez EA, Taha-Tijerina J. Nanotechnology applications for electrical transformers—A review. *Electric Power Systems Research*. 2017;**143**:573-584
- [4] Kumar MS, Das AP. Emerging nanotechnology based strategies for diagnosis and therapeutics of urinary tract infections: A review. *Advances in Colloid and Interface Science*. 2017;**249**:53-65
- [5] Iavicoli I, Leso V, Beezhold DH, Shvedova AA. Nanotechnology in agriculture: Opportunities, toxicological implications, and occupational risks. *Toxicology and Applied Pharmacology*. 2017;**329**:96-111
- [6] Hussein AK. Applications of nanotechnology to improve the performance of solar collectors-recent advances and overview. *Renewable and Sustainable Energy Reviews*. 2016;**62**:767-792
- [7] Kasaeian A, Eshghi AT, Sameti M. A review on the applications of nanofluids in solar energy systems. *Renewable and Sustainable Energy Reviews*. 2015;**43**:584-598
- [8] Mihindukulasuriya SDF, Lim LT. Nanotechnology development in food packaging: A review. *Trends in Food Science & Technology*. 2014;**40**(2):149-167
- [9] Gupta MC, Ungaro C, Foley JJ, Gray SK. Optical nanostructures design, fabrication, and applications for solar/thermal energy conversion. *Solar Energy*. 2018;**165**:100-114
- [10] Jagadale SB, Patil VL, Vanalakar SA, Patil PS, Deshmukh HP. Preparation, characterization of 1D ZnO nanorods and their gas sensing properties. *Ceramics International*. 2018;**44**(3):3333-3340
- [11] Leitner J, Bartůněk V, Sedmidubský D, Jankovský O. Thermodynamic properties of nanostructured ZnO. *Applied Materials Today*. 2018;**10**:1-11
- [12] Chongsri K, Boonyarattanakalin K, Pecharapa W. Effects of seeding layer thickness on physical and morphological structure of Ga/F co-doped ZnO nanostructures. *Materials Today: Proceedings*. 2017;**4**(5, Part 2):6129-6133
- [13] Qi B, Ólafsson S, Gíslason HP. Vacancy defect-induced d0 ferromagnetism in undoped ZnO nanostructures: Controversial origin and challenges. *Progress in Materials Science*. 2017;**90**:45-74
- [14] Buller S, Strunk J. Nanostructure in energy conversion. *Journal of Energy Chemistry*. 2016;**25**(2):171-190
- [15] Tereshchenko A, Bechelany M, Viter R, Khranovskyy V, Smyntyna V, Starodub N, et al. Optical biosensors based on ZnO nanostructures: Advantages and perspectives. A review. *Sensors and Actuators B: Chemical*. 2016;**229**:664-677
- [16] Maçaira J, Andrade L, Mendes A. Review on nanostructured photoelectrodes for next generation dye-sensitized solar cells. *Renewable and Sustainable Energy Reviews*. 2013;**27**:334-349

- [17] Spencer MJS. Gas sensing applications of 1D-nanostructured zinc oxide: Insights from density functional theory calculations. *Progress in Materials Science*. 2012;**57**(3):437-486
- [18] Ramos-Ramón JA, Pal U, Cremades A, Maestre D. Effect of Ga incorporation on morphology and defect structures evolution in VLS grown 1D  $\text{In}_2\text{O}_3$  nanostructures. *Applied Surface Science*. 2018;**439**:1010-1018
- [19] Huang PS, Gao TC. Current development of 1D and 2D metallic nanomaterials for the application of transparent conductors in solar cells: Fabrication and modeling. *Nano-Structures & Nano-Objects*. 2018;**15**:119-139
- [20] Terasako T, Kohno K, Yagi M. Vapor-liquid-solid growth of  $\text{SnO}_2$  nanowires utilizing alternate source supply and their photoluminescence properties. *Thin Solid Films*. 2017;**644**:3-9
- [21] Mijangos C, Hernández R, Martín J. A review on the progress of polymer nanostructures with modulated morphologies and properties, using nanoporous AAO templates. *Progress in Polymer Science*. 2016;**54-55**:148-182
- [22] Kente T, Mhlanga SD. Gallium nitride nanostructures: Synthesis, characterization and applications. *Journal of Crystal Growth*. 2016;**444**:55-72
- [23] Gaikwad MA, Suryawanshi MP, Maldar PS, Dongale TD, Moholkar AV. Nanostructured zinc oxide photoelectrodes by green routes M-SILAR and electrodeposition for dye sensitized solar cell. *Optical Materials*. 2018;**78**:325-334
- [24] Tabrizi AG, Arsalani N, Namazi H, Ahadzadeh I. Vanadium oxide assisted synthesis of polyaniline nanoarrays on graphene oxide sheets and its application in supercapacitors. *Journal of Electroanalytical Chemistry*. 2017;**798**:34-41
- [25] Mirzaei A, Neri G. Microwave-assisted synthesis of metal oxide nanostructures for gas sensing application: A review. *Sensors and Actuators B: Chemical*. 2016;**237**:749-775
- [26] Tsega M, Kuo DH, Dejene FB. Growth and green defect emission of  $\text{ZnPbO}$  nanorods by a catalyst-assisted thermal evaporation-oxidation method. *Journal of Crystal Growth*. 2015;**415**:106-110
- [27] Mukasyan AS, Rogachev AS, Aruna ST. Combustion synthesis in nanostructured reactive systems. *Advanced Powder Technology*. 2015;**26**(3):954-976
- [28] Bueno C, Maestre D, Díaz T, Juárez H, Pacio M, Cremades A, et al. High-yield growth of Ti doped ZnO nano- and microstructures by a vapor-solid method. *Journal of Alloys and Compounds*. 2017;**726**:201-208
- [29] Nersisyan HH, Lee JH, Ding JR, Kim KS, Manukyan KV, Mukasyan AS. Combustion synthesis of zero-, one-, two- and three-dimensional nanostructures: Current trends and future perspectives. *Progress in Energy and Combustion Science*. 2017;**63**:79-118
- [30] Balela MDL, Acedera RA, Flores CLI, Pelicano CMO. Surface modification of ZnO nanostructured film prepared by hot water oxidation. *Surface and Coatings Technology*. 2018;**340**:199-209
- [31] Alinauskas L, Brooke E, Regoutz A, Katelnikovas A, Raudonis R, Yitzchaik S, et al. Nanostructuring of  $\text{SnO}_2$  via solution-based and hard template assisted method. *Thin Solid Films*. 2017;**626**:38-45

- [32] Veluswamy P, Sathiyamoorthy S, Chowdary KH, Muthusamy O, Krishnamoorthy K, Takeuchi T, et al. Morphology dependent thermal conductivity of ZnO nanostructures prepared via a green approach. *Journal of Alloys and Compounds*. 2017;**695**:888-894
- [33] Montazerzohori M, Masoudiasl A, Doert T. Two new 1D zigzag Hg(II) nanostructure coordination polymers: Sonochemical synthesis, thermal study, crystal structure and Hirshfeld surface analysis. *Inorganica Chimica Acta*. 2016;**443**:207-217
- [34] Doganay D, Coskun S, Kaynak C, Unalan HE. Electrical, mechanical and thermal properties of aligned silver nanowire/polylactide nanocomposite films. *Composites Part B: Engineering*. 2016;**99**:288-296
- [35] Ghosh S, Dev BN. Probing of O<sub>2</sub> vacancy defects and correlated magnetic, electrical and photoresponse properties in indium-tin oxide nanostructures by spectroscopic techniques. *Applied Surface Science*. 2018;**439**:891-899
- [36] Paek J, Kim J, An BW, Park J, Ji S, Kim SY, et al. Stretchable electronic devices using graphene and its hybrid nanostructures. *FlatChem*. 2017;**3**:71-91
- [37] Matysiak W, Tański T, Zaborowska M. Manufacturing process, characterization and optical investigation of amorphous 1D zinc oxide nanostructures. *Applied Surface Science*. 2018;**442**:382-389
- [38] Abdeltwab E, Taher FA. Polar and nonpolar self-assembled Co-doped ZnO thin films: Structural and magnetic study. *Thin Solid Films*. 2017;**636**:200-206
- [39] Thiebaud L, Legeai S, Stein N. Tuning the morphology of Te one-dimensional nanostructures by template-free electrochemical deposition in an ionic liquid. *Electrochimica Acta*. 2016;**197**:300-306
- [40] Vadivel S, Naveen AN, Theerthagiri J, Madhavan J, Priya TS, Balasubramanian N. Solvothermal synthesis of BiPO<sub>4</sub> nanorods/ MWCNT (1D-1D) composite for photocatalyst and supercapacitor applications. *Ceramics International*. 2016;**42**(12):14196-14205
- [41] Pal B, Dhara S, Giri PK, Sarkar D. Evolution of room temperature ferromagnetism with increasing 1D growth in Ni-doped ZnO nanostructures. *Journal of Alloys and Compounds*. 2015;**647**:558-565
- [42] Ghosh R, Das R, Giri PK. Label-free glucose detection over a wide dynamic range by mesoporous Si nanowires based on anomalous photoluminescence enhancement. *Sensors and Actuators B: Chemical*. 2018;**260**:693-704
- [43] Chandola S, Speiser E, Esser N, Appelfeller S, Franz M, Dähne M. Optical anisotropy of quasi-1D rare-earth silicide nanostructures on Si(001). *Applied Surface Science*. 2017;**399**:648-653
- [44] Maryasin V, Bucci D, Rafhay Q, Panicco F, Michallon J, Kaminski-Cachopo A. Technological guidelines for the design of tandem III-V nanowire on Si solar cells from opto-electrical simulations. *Solar Energy Materials and Solar Cells*. 2017;**172**:314-323
- [45] Legesse M, Fagas G, Nolan M. Modifying the band gap and optical properties of germanium nanowires by surface termination. *Applied Surface Science*. 2017;**396**:1155-1163
- [46] Vishnukumar P, Vivekanandhan S, Misra M, Mohanty AK. Recent advances and emerging opportunities in phytochemical synthesis of ZnO nanostructures. *Materials Science*



in Semiconductor Processing.  
 2018;**80**:143-161

[47] Vittal R, Ho KC. Zinc oxide based dye-sensitized solar cells: A review. *Renewable and Sustainable Energy Reviews*. 2017;**70**:920-935

[48] Ghoderao KP, Jamble SN, Kale RB. Influence of pH on hydrothermally derived ZnO nanostructures. *Optik*. 2018;**156**:758-771

[49] Huang MH, Wu YY, Feick H, Tran N, Weber E, Yang PD. Catalytic growth of zinc oxide nanowires by vapor transport. *Advanced Materials*. 2001;**13**(2):113-116

[50] Huang MH, Mao S, Feick H, Yan HQ, Wu YY, Kind H, et al. Room-temperature ultraviolet nanowire nanolasers. *Science*. 2001;**292**:1897-1899

[51] Alsultany FH, Hassan Z, Ahmed NM, Almessiere MA. Catalytic growth of one-dimensional single-crystalline ZnO nanostructures on glass substrate by vapor transport. *Ceramics International*. 2017;**43**:610-616

[52] Athma PV, Martinez AI, Johns N, Safeera TA, Reshmi R, Anila EI. Nanostructured zinc oxide thin film by simple vapor transport deposition. *Superlattices and Microstructures*. 2015;**85**:379-384

[53] Hosseini ZS, Mortezaali A, Iraj Zad A. Comparative study of the grown ZnO nanostructures on quartz and alumina substrates by vapor phase transport method without catalyst: Synthesis and acetone sensing properties. *Sensors and Actuators A*. 2014;**212**:80-86

[54] Babu ES, Kim SJ, Song JH, Hong SK. Effects of growth pressure on morphology of ZnO nanostructures by chemical vapor transport. *Chemical Physics Letters*. 2016;**658**:182-187

[55] Trad TM, Donley KB, Look DC, Eyink KG, Tomich DH, Taylor CR. Low

temperature deposition of zinc oxide nanoparticles via zinc-rich vapor phase transport and condensation. *Journal of Crystal Growth*. 2010;**312**:3675-3679

[56] Haldar SR, Nayak A, Chini TK, Bhunia S. Strong temperature and substrate effect on ZnO nanorod flower structures in modified chemical vapor condensation growth. *Current Applied Physics*. 2010;**10**:942-946

[57] Pan ZW, Dai ZR, Wang ZL. Nanobelts of semiconducting oxides. *Science*. 2001;**291**:1947-1949

[58] Tonezzer M, Dang TTL, Bazzanella N, Nguyen VH, Iannotta S. Comparative gas-sensing performance of 1D and 2D ZnO nanostructures. *Sensors and Actuators B: Chemical*. 2015;**220**:1152-1160

[59] Manthina V, Agrios AG. Single-pot ZnO nanostructure synthesis by chemical bath deposition and their applications. *Nano-Structures & Nano-Objects*. 2016;**7**:1-11

[60] Bakhsheshi-Rad HR, Hamzah E, Ismail AF, Aziz M, Kasiri-Asgarani M, Akbari E, et al. Synthesis of a novel nanostructured zinc oxide/baghdadite coating on Mg alloy for biomedical application: *In-vitro* degradation behavior and antibacterial activities. *Ceramics International*. 2017;**43**:14842-14850

[61] Shirahata T, Kawaharamura T, Fujita S, Orita H. Transparent conductive zinc-oxide-based films grown at low temperature by mist chemical vapor deposition. *Thin Solid Films*. 2015;**597**:30-38

[62] Laurenti M, Garino N, Porro S, Fontana M, Gerbaldi C. Zinc oxide nanostructures by chemical vapour deposition as anodes for Li-ion batteries. *Journal of Alloys and Compounds*. 2015;**640**:321-326

- [63] Menzel A, Subannajui K, Bakhda R, Wang YB, Thomann R, Zacharias M. Tuning the growth mechanism of ZnO nanowires by controlled carrier and reaction gas modulation in thermal CVD. *The Journal of Physical Chemistry Letters*. 2012;**3**:2815-2821
- [64] Park WI, Kim DH, Jung SW, Yi GC. Metalorganic vapor-phase epitaxial growth of vertically well-aligned ZnO nanorods. *Applied Physics Letters*. 2002;**80**(22):4232-4234
- [65] Wu YF, Liu DP, Yu NS, Liu YD, Liang HW, Du GT. Structure and electrical characteristics of zinc oxide thin films grown on Si (111) by metal-organic chemical vapor deposition. *Journal of Materials Science and Technology*. 2013;**29**(9):830-834
- [66] Kim AY, Jang SS, Lee DH, Yim SY, Byun DJ. Effects of temperature on ZnO hybrids grown by metal-organic chemical vapor deposition. *Materials Research Bulletin*. 2012;**47**:2888-2890
- [67] Torres-Huerta AM, Domínguez-Crespo MA, Brachetti-Sibaja SB, Arenas-Alatorre J, Rodríguez-Pulido A. Effect of the substrate on the properties of ZnO–MgO thin films grown by atmospheric pressure metal-organic chemical vapor deposition. *Thin Solid Films*. 2011;**519**:6044-6052
- [68] Fragalà ME, Aleeva Y, Malandrino G. Effects of metal-organic chemical vapour deposition grown seed layer on the fabrication of well aligned ZnO nanorods by chemical bath deposition. *Thin Solid Films*. 2011;**519**:7694-7701
- [69] Wu CL, Chang L, Chen HG, Lin CW, Chang TF, Chao YC, et al. Growth and characterization of chemical-vapor-deposited zinc oxide nanorods. *Thin Solid Films*. 2006;**498**:137-141
- [70] Vallejos S, Gràcia I, Lednický T, Vojkuvka L, Figueras E, Hubálek J, et al. Highly hydrogen sensitive micromachined sensors based on aerosol-assisted chemical vapor deposited ZnO rods. *Sensors and Actuators B*. 2018;**268**:15-21
- [71] Chandrasekhar KR, Arbuj SS. Solvothermal synthesis of one dimensional ZnO nanostructures and its photocatalytic applications. *Materials Today: Proceedings*. 2015;**2**(9, Part 1)
- [72] Badnore AU, Pandit AB. Effect of pH on sonication assisted synthesis of ZnO nanostructures: Process details. *Chemical Engineering and Processing Process Intensification*. 2017;**122**:235-244
- [73] Colorado SA, Colorado HA. Manufacturing of zinc oxide structures by thermal oxidation processes as scalable methods towards inexpensive electric generators. *Ceramics International*. 2017;**43**:15846-15855
- [74] Hong SH, Kim MH, Yun HW, Paik TJ, Lee H. Solution-processed fabrication of superhydrophobic hierarchical zinc oxide nanostructures *via* nanotransfer printing and hydrothermal growth. *Surface & Coatings Technology*. 2017;**331**:189-195
- [75] Chen RQ, Zou CW, Yan XD, Gao W. Zinc oxide nanostructures and porous films produced by oxidation of zinc precursors in wet-oxygen atmosphere. *Progress in Natural Science: Materials International*. 2011;**21**:81-96
- [76] Kumarakuru H, Urgessa ZN, Olivier EJ, Botha JR, Venter A, Neethling JH. Growth of ZnS-coated ZnO nanorod arrays on (100) silicon substrate by two-step chemical synthesis. *Journal of Alloys and Compounds*. 2014;**612**:154-162
- [77] Sinha D, De D, Goswami D, Ayaz A. Fabrication of DSSC with nanostructured ZnO photo anode and

natural dye sensitizer. *Materials Today: Proceedings*. 2018;5(1, Part 2):2056-2063

nanowires with CdSe quantum dots for photovoltaic devices. *Nano Letters*. 2007;7(6):1793-1798

[78] Marimuthu T, Anandhan N, Thangamuthu R. Electrochemical synthesis of one-dimensional ZnO nanostructures on ZnO seed layer for DSSC applications. *Applied Surface Science*. 2018;428:385-394

[86] Xu YF, Wu WQ, Rao HS, Chen HY, Kuang DB, Su CY. CdS/CdSe co-sensitized TiO<sub>2</sub> nanowire-coated hollow spheres exceeding 6% photovoltaic performance. *Nano Energy*. 2015;11:621-630

[79] Nayeri FD, Akbarnejad E, Ghoranneviss M, Soleimani EA, Hashemizadeh SA. Dye decorated ZnO-NWs/CdS-NPs heterostructures for efficiency improvement of quantum dots sensitized solar cell. *Superlattices and Microstructures*. 2016;91:244-251

[87] Sun JK, Jiang Y, Zhong XH, Hu JS, Wan LJ. Three-dimensional nanostructured electrodes for efficient quantum-dot-sensitized solar cells. *Nano Energy*. 2017;32:130-156

[80] Eskandari M, Ahmadi V, Kohnehpoushi S, Yousefi rad M. Improvement of ZnO nanorod based quantum dot (cadmium sulfide) sensitized solar cell efficiency by aluminum doping. *Physica E: Low-dimensional Systems and Nanostructures*. 2015;66:275-282

[88] Majumder T, Dhar S, Chakraborty P, Debnath K, Mondal SP. Advantages of ZnO nanotaper photoanodes in photoelectrochemical cells and graphene quantum dot sensitized solar cell applications. *Journal of Electroanalytical Chemistry*. 2018;813:92-101

[81] Rawal SB, Sung SD, Moon SY, Shin YJ, Lee WI. Optimization of CdS layer on ZnO nanorod arrays for efficient CdS/CdSe co-sensitized solar cell. *Materials Letters*. 2012;82:240-243

[82] Li L, Zhai TY, Bando Y, Golberg D. Recent progress of one-dimensional ZnO nanostructured solar cells. *Nano Energy*. 2012;1(1):91-106

[83] Sharma D, Jha R, Kumar S. Quantum dot sensitized solar cell: Recent advances and future perspectives in photoanode. *Solar Energy Materials and Solar Cells*. 2016;155:294-322

[84] Jafarzadeh M, Sipaut CS, Dayou J, Mansa RF. Recent progresses in solar cells: Insight into hollow micro/nano-structures. *Renewable and Sustainable Energy Reviews*. 2016;64:543-568

[85] Leschkies KS, Divakar R, Basu J, Enache-Pommer E, Boercker JE, Carter CB, et al. Photosensitization of ZnO